

ENSO and greenhouse warming

Wenju Cai^{1,2*}, Agus Santoso³, Guojian Wang¹, Sang-Wook Yeh⁴, Soon-Il An⁵, Kim M. Cobb⁶, Mat Collins⁷, Eric Guilyardi^{8,9}, Fei-Fei Jin¹⁰, Jong-Seong Kug¹¹, Matthieu Lengaigne⁸, Michael J. McPhaden¹², Ken Takahashi¹³, Axel Timmermann¹⁴, Gabriel Vecchi¹⁵, Masahiro Watanabe¹⁶ and Lixin Wu²

The El Niño/Southern Oscillation (ENSO) is the dominant climate phenomenon affecting extreme weather conditions worldwide. Its response to greenhouse warming has challenged scientists for decades, despite model agreement on projected changes in mean state. Recent studies have provided new insights into the elusive links between changes in ENSO and in the mean state of the Pacific climate. The projected slow-down in Walker circulation is expected to weaken equatorial Pacific Ocean currents, boosting the occurrences of eastward-propagating warm surface anomalies that characterize observed extreme El Niño events. Accelerated equatorial Pacific warming, particularly in the east, is expected to induce extreme rainfall in the eastern equatorial Pacific and extreme equatorward swings of the Pacific convergence zones, both of which are features of extreme El Niño. The frequency of extreme La Niña is also expected to increase in response to more extreme El Niños, an accelerated maritime continent warming and surface-intensified ocean warming. ENSO-related catastrophic weather events are thus likely to occur more frequently with unabated greenhouse-gas emissions. But model biases and recent observed strengthening of the Walker circulation highlight the need for further testing as new models, observations and insights become available.

The impacts of anthropogenic climate change may be felt through changes in modes of natural climatic variability. ENSO is the most important year-to-year fluctuation of the climate system on the planet¹, varying between anomalously cold (La Niña) and warm (El Niño) conditions. Underpinning occurrences of ENSO events is the positive feedback between trade wind intensity and zonal contrasts in sea surface temperature (SST), referred to as the Bjerknes feedback. The trade winds normally pile up warm surface water in the western Pacific while upwelling colder subsurface water in the east along the equator and off the west coast of South America. The resulting east–west surface temperature contrast reinforces an east–west air pressure difference across the basin that in turn drives the trade winds. During La Niña, the system strengthens, but during El Niño, the trade winds weaken as atmospheric pressure rises in the western Pacific and falls in the eastern Pacific. The Bjerknes feedback now operates in reverse, with weakened trade winds and SST warming tendencies along the Equator reinforcing one another. It is still not clear what sets this quasi-oscillatory behaviour, that is, whether ENSO is self-sustaining or triggered by stochastic forcing². What is clear is that ocean and atmosphere preconditions are required³, as supported by the fundamental characteristics of the mean tropical climate such as thermal gradients and associated circulations that balance radiative heating⁴. These swings in temperature are accompanied by changes in the structure of the subsurface ocean, the position of atmospheric convection and associated global teleconnection patterns, severely disrupting global weather patterns^{5–10}, and affecting ecosystems¹¹ and agriculture¹² worldwide.

During the 1982/1983 and 1997/1998 extreme El Niño events^{6,8}, surface warming anomalies propagated eastward in an uncharacteristic fashion^{13,14}, and massive surface warm anomalies in the eastern equatorial Pacific exceeding 3 °C caused an equatorward shift of the Intertropical Convergence Zone (ITCZ). Catastrophic floods occurred in the eastern equatorial region of Ecuador and northern Peru^{6,8}. The South Pacific Convergence Zone (SPCZ), the largest rain band in the Southern Hemisphere, shifted equatorward by up to 1,000 km (an event referred to as zonal SPCZ¹⁰), spurring floods and droughts in south Pacific countries and shifting extreme cyclones to regions normally not affected by such events¹⁰. Other impacts included floods in the southwest United States, disappearance of marine life, and decimation of the native bird population in the Galapagos Islands¹⁵. The development of the 1997/1998 extreme El Niño event was accompanied by an extreme positive Indian Ocean Dipole in boreal autumn, affecting millions of people across countries in the Indian Ocean rim. An extreme La Niña ensued in 1998/1999, generating droughts in the southwest United States and eastern equatorial Pacific regions, floods in the western Pacific and central American countries, and increased land-falling west Pacific tropical cyclones and Atlantic hurricanes^{7,9,12}.

In light of these massive impacts, how ENSO will respond to greenhouse warming is one of the most important issues in climate change science. The issue has challenged scientists for decades, but there has been no consensus on how ENSO amplitude and frequency may change^{16–18}. Past studies have proceeded without specifically looking into the response of ENSO extremes, and

¹CSIRO Oceans and Atmosphere Flagship, Aspendale, Victoria 3195, Australia. ²Physical Oceanography Laboratory, Qingdao Collaborative Innovation Center of Marine Science and Technology, Ocean University of China, Qingdao 266003, China. ³Australian Research Council (ARC) Centre of Excellence for Climate System Science and Climate Change Research Centre, Level 4 Mathews Building, The University of New South Wales, Sydney 2052, Australia.

⁴Department of Environmental Marine Science, Hanyang University, Ansan 426-791, South Korea. ⁵Department of Atmospheric Sciences, Yonsei University, Seoul 120-749, South Korea. ⁶School of Earth & Atmospheric Sciences, Georgia Institute of Technology, 311 Ferst Drive, Atlanta 30332-0340, USA. ⁷College of Engineering Mathematics and Physical Sciences, Harrison Building, Streatham Campus, University of Exeter, Exeter EX1 3PB, UK.

⁸Laboratoire d'Océanographie et du Climat: Expérimentation et Approches Numériques (LOCEAN), IRD/UPMC/CNRS/MNHN, Paris Cedex 05, France.

⁹NCAS-Climate, University of Reading, Reading RG6 6BB, UK. ¹⁰Department of Meteorology, SOEST, University of Hawaii, Honolulu, Hawaii 96822, USA.

¹¹School of Environmental Science & Engineering, Pohang University of Science and Technology, Pohang 790-784, South Korea. ¹²NOAA/Pacific Marine Environmental Laboratory, Seattle, Washington 98115, USA. ¹³Instituto Geofísico del Perú, Lima 169, Perú. ¹⁴IPRC, Department of Oceanography, SOEST, University of Hawaii, Honolulu, Hawaii 96822, USA. ¹⁵Geophysical Fluid Dynamics Laboratory/NOAA, Princeton, New Jersey 08540-6649, USA.

¹⁶Atmosphere and Ocean Research Institute, University of Tokyo, Kashiwa 277-8564, Japan. *e-mail: wenju.cai@csiro.au

have focused on simple metrics such as temperature variability in the eastern equatorial Pacific and linear dynamics, assuming that the characteristics of El Niño and La Niña are symmetric. Through the Coupled Model Intercomparison Phase 5 (CMIP5) process¹⁹, substantial improvement in modelling ENSO has been made^{18,20,21}. There is recognition that the two opposing extremes are not mirror opposites^{13,22–27}; that is, the impacts of and processes responsible for extreme El Niño and La Niña events are not symmetric^{14,28–32}. Further, the dynamics of extreme ENSO events are different from moderate events^{14,31–33}, and therefore the two must be examined separately in terms of their response to greenhouse warming.

With this recognition, significant progress has been made in understanding the characteristics of extreme ENSO events in models and observations, as part of the observed diversity of events, such as central Pacific ENSO^{33–35} or ENSO Modoki³⁶, their likely future behaviour under greenhouse conditions, and potential changes in their teleconnections. This study provides a review of these advances. We show that the frequency of ENSO extremes is expected to increase, ENSO teleconnections are likely to shift eastward, and these changes can, to a large extent, be interpreted as consequences of mean state changes.

Changes in the mean state

The dynamics and properties of ENSO are closely linked to the slowly evolving background climate state of the equatorial Pacific Ocean (for example by rectifying into the mean state^{37,38}), which in turn affects ENSO feedback processes^{1,16}. The tropical Pacific is projected to change under greenhouse warming. The projection (Box 1) includes a weakening of the Walker circulation^{39–41}, a faster warming rate in the equatorial than off-equatorial Pacific^{16,39,41}, in the eastern equatorial Pacific⁴¹ and the Maritime continent than in the central Pacific, and over the ocean surface than subsurface^{32,42}. The warming pattern gives rise to an increase in rainfall in the equatorial Pacific, particularly in the eastern part of the basin⁴³.

Despite a strong intermodel agreement, there is vigorous debate as to the causes of, and the confidence in, these projected mean state changes. The Walker circulation is expected to weaken because tropical precipitation increases at a slower rate than water vapour, so the tropical atmospheric overturning must slow down with weaker equatorial trade winds, and would occur even without a change in the west-minus-east SST gradient⁴⁰. Observations show a weakening over the past six decades (1950–2009) but this was accompanied by a weakening in the west-minus-east SST gradient in the Indo-Pacific⁴⁴, suggesting a coupling between oceanic and atmospheric changes. Such coupling would imply that future changes of the Walker circulation need not be static or unidirectional^{18,45} and could be influenced, for instance, by a differential warming between the Pacific and other oceanic basins. For example, a strengthening Walker circulation can be associated with a faster warming in the Indian Ocean^{18,46} or the Atlantic⁴⁷.

Another point of contention is that, in stark contrast to the projection, the Walker circulation has strengthened over the past three decades^{48–51}. The observed strengthening is suggested to play a role in the so-called ‘global warming hiatus’^{50,52}, but there is debate as to its mechanism. One contributing factor could be the negative phase of Interdecadal Pacific Oscillation (IPO)⁵⁰ as signified by a massive sea-level rise in the western tropical Pacific⁵³. The other could be decadal variations in ENSO properties, for instance a random string of La Niña events⁵⁴, or a lack of strong eastern Pacific El Niño events⁵⁵ but more frequent central Pacific El Niños⁵⁴ facilitated by the warmer western Pacific mean state⁵⁶. But the interdecadal fluctuations in ENSO properties and the IPO themselves may be interrelated, given that ENSO rectification can be a mechanism for interdecadal mean state changes^{37,38}.

The projected mean state changes are expected to modify ENSO’s amplifying and damping feedbacks. The net change in feedbacks has

been found to vary considerably across models, contributing to a lack of consensus in the change of ENSO SST variability^{16–18}. The increased vertical temperature gradient, caused by a surface-intensified ocean warming, would enhance the Ekman pumping feedback that tends to increase variability in the central Pacific³². The weakened easterly trade winds would lead to an anomalous net poleward transport of warm water¹⁶, causing the depth of the mean equatorial thermocline to shoal. This can enhance the thermocline feedback through an increased sensitivity to wind variability¹⁸, despite being partially offset by a reduction in mean upwelling associated with the weaker mean easterly winds. Surface warming enhances evaporation and cloud cover, leading to a reduction in shortwave radiation, thus increasing the efficiency of thermodynamic damping that weakens El Niño growth¹⁶, although uncertainties remain because models still struggle to represent the observed relationships²¹. This delicate balance between damping and amplifying feedback processes is vastly different across models^{16–18,21}. When only models with a better representation of the various linear feedbacks are considered, an intermodel consensus in the temporal evolution of ENSO SST amplitude response is achieved¹⁸: the models show an increased variability before the year 2040, when SST warms faster in the eastern Pacific Ocean than over the maritime region, but decreasing variability thereafter, when the latter warms more rapidly.

The notion that ENSO properties are affected by the mean state changes seems to be supported by observations and theory^{57,58}. The mid-1970 shift of the IPO from a colder to a warmer tropical eastern Pacific saw a stronger ENSO amplitude⁵⁸, marked by the 1988/1989 and 1998/1999 extreme La Niña events, which were characterized by reduced atmospheric convection in the central Pacific³², and the 1982/1983 and 1997/1998 extreme El Niño, which featured eastward-propagating SST anomalies^{13,14}, a shift of the ITCZ to the eastern equatorial Pacific³ and a zonal SPCZ event¹⁰. Since the early 2000s, the colder eastern equatorial Pacific saw reduced ENSO SST variability in the eastern Pacific but increased SST variability in the central Pacific²⁵. The asymmetric features between extreme La Niña and extreme El Niño, and the vastly different changes in ENSO SST variability at different longitudes, also suggest that an examination of a change in ENSO properties must move away from using only one index at a fixed location, and must take into account spatial asymmetry of ENSO anomalies.

ENSO asymmetry and extremes

El Niño and La Niña events are not symmetric in spatial pattern^{22–24,59} or temporal evolution^{13,60,61}. Extreme El Niño features disproportionately warm maximum SST anomalies in the eastern equatorial Pacific, but the anomaly centres of weak El Niño and extreme La Niña events are situated in the central equatorial Pacific²⁵. The anomaly centre of weak La Niña is located further towards the eastern equatorial Pacific than extreme La Niña^{25,26,31,32}. This spatial asymmetry is characterized by positive SST skewness in the eastern equatorial Pacific, but negative skewness in the central equatorial Pacific⁶². In addition, an extreme La Niña tends to follow an extreme El Niño^{27,32}, but not the other way around. A La Niña can last for more than a year, whereas El Niño events tend to terminate abruptly in late boreal winter or spring^{13,60,61}.

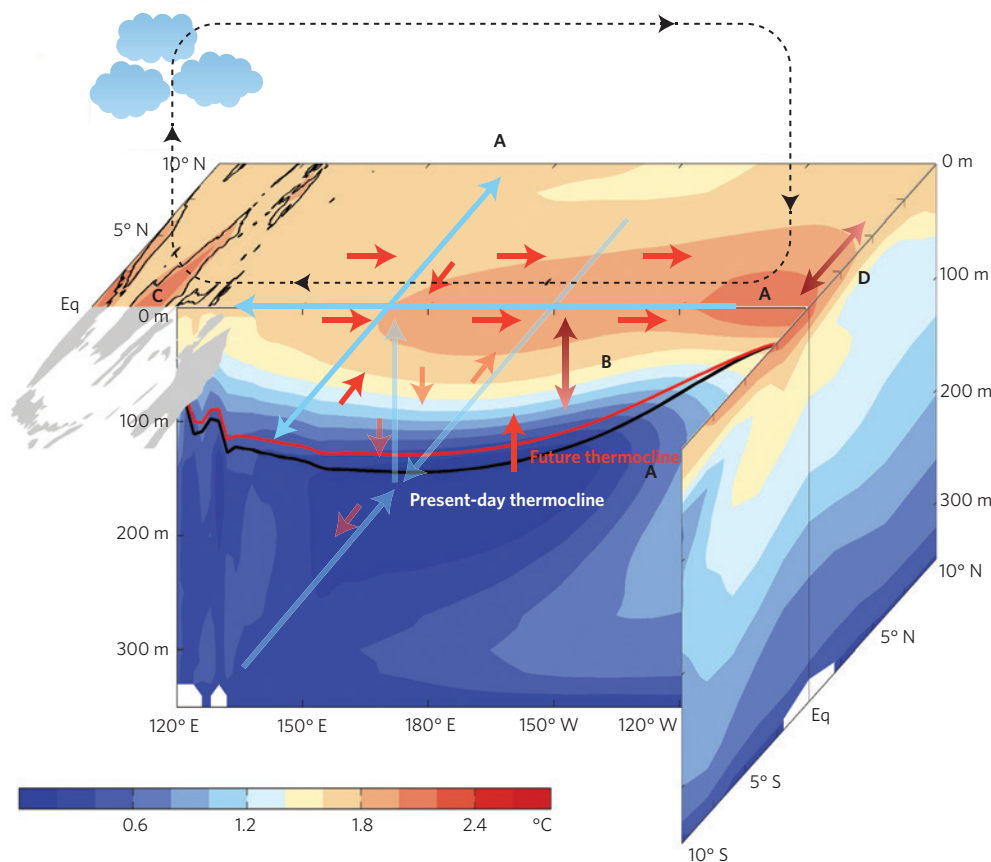
The asymmetries require at least two ENSO indices to distinguish extreme El Niño from extreme La Niña, or extreme El Niño from weak El Niño^{25,26,31,32}. The two indices may be obtained by empirical orthogonal function (EOF) analysis of SST anomalies, which deconvolves the spatiotemporal SST variability into orthogonal modes, each described by a principal spatial pattern and the corresponding principal component (PC) time series. An event may be described by an appropriately weighted superposition of the two modes. One EOF depicts strong variability in the Niño3.4 or Niño3 region²⁵ (Fig. 1a) and the other resembles the central Pacific El Niño pattern^{34–36} (Fig. 1b). An extreme El Niño (red stars,

Box 1 | Mean state changes and consequences.

Features associated with a weakening Walker circulation (A). The trade winds and equatorial currents weaken, the eastern equatorial Pacific warms faster than the surrounding regions, and the thermocline shallows (present-day, black curve; future, red curve). The weakening equatorial zonal currents are conducive to an increased frequency of eastward-propagating El Niño events. The faster warming in the eastern equatorial Pacific is favourable for an increased frequency of extreme El Niño events by promoting atmospheric convection. The increased occurrences of extreme El Niño are in turn conducive to an increased frequency of La Niña owing to a discharged thermocline that promotes an influence of the subsurface cool water in the central Pacific.

Increasing vertical temperature gradients (B) and enhanced warming (C) over the maritime continent. These changes are additional factors that help to produce an increased frequency of extreme La Niña events, through nonlinear zonal advection and Ekman pumping.

Accelerated warming (D) in the equatorial rather than in the off-equatorial Pacific. This change leads to an increased frequency of equatorward shifts of the ITCZ, which characterizes an extreme El Niño, and to an increased frequency of extreme swings of the SPCZ towards the Equator. This occurs because atmospheric convection tends to follow maximum sea surface temperatures.



The schematic figure shows greenhouse-induced future changes at the surface (shown only for the north Pacific) and upper-ocean along-Equator and meridional cross-sections. Greenhouse-induced changes (red arrows) to the mean Walker circulation (dashed black arrows) and mean ocean currents (cyan arrows) are indicated. Main features of changes are indicated by letters A, B, C and D.

Fig. 1c,f) is described by the difference between EOF1 and EOF2, or an E-index defined as $(PC1 - PC2)/\sqrt{2}$ (ref. 25), corresponding to extreme positive SST anomalies in the eastern equatorial Pacific (Niño3 region, Fig. 1e). An extreme La Niña (blue stars, Fig. 1c) is described by the sum of EOF1 and EOF2, or a large C-index defined as $(PC1+PC2)/\sqrt{2}$ (Fig. 1d) (ref. 25), giving rise to maximum cooling in the central Pacific (Fig. 1h,i) and can be represented by SST anomalies in the Niño4 region (Fig. 1d).

Despite the recognition of inter-event differences⁶³, debates persist as to whether the central Pacific El Niño^{34,35}, whose spatial pattern resembles EOF2, is part of the ENSO asymmetry^{25,26} or a distinct mode³⁶. Several arguments support the view of the former.

First, EOF2 is a ‘modulator’ for describing inter-event differences, and it rarely appears without a substantial projection onto EOF1. Many central Pacific El Niño events (Fig. 1g; purple dots in Fig. 1c, defined as when the C-index is greater than one standard deviation, s.d.) have a considerable contribution from EOF2, like La Niña events (Fig. 1d) but with an opposite sign. Even weak El Niño events (yellow dots, Fig. 1c) involve both EOFs (Fig. 1c), and together they represent a ‘continuum’³³. Indeed, warm and cold events occur over a broad range of longitudes, but their anomaly centres co-mingle³³. Second, the anomaly patterns of the central Pacific El Niño and extreme La Niña are somewhat similar, and both can be represented by Niño4 (Fig. 1d). It is extreme El Niño events (red stars, Fig. 1c)

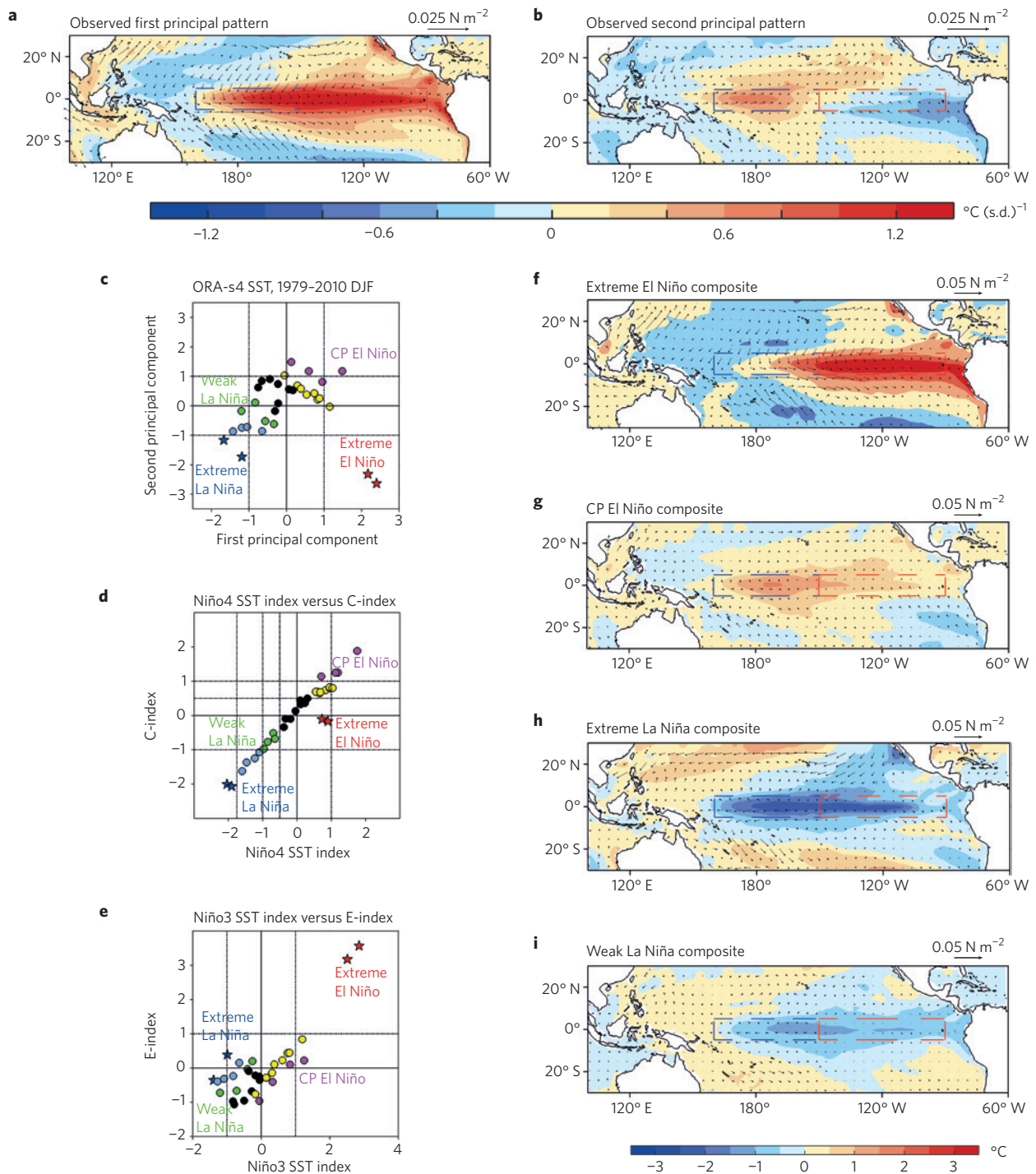


Figure 1 | Observed ENSO asymmetry. **a, b**, First and second principal variability patterns of SST obtained by applying EOF analysis to satellite-era SST anomalies in austral summer (DJF), in the tropical Pacific region of 15° S to 15° N, 140° E–80° W. The SST anomalies and wind stress vectors are presented as linear regression onto standardized PC time series. **c**, Relationship between the two principal component time series. **d**, Relationship between C-index and Niño4 SST index (160° E to 150° W, 5° S to 5° N, indicated by the blue box in each panel). **e**, Relationship between E-index and Niño3 SST index (150–90° W, 5° S to 5° N, indicated by the red box in each panel). Blue stars indicate extreme La Niña events, that is, 1988/1989 and 1998/1999, defined as when both principal components are negative but greater than 1 s.d. in amplitude (as shown in panel **c**), or quadratically detrended Niño4 is negative but greater than 1.75 s.d. in amplitude (as shown in **d**); light blue dots indicate moderate La Niña events, that is, 1983/84, 1999/00, 2007/08 and 2010/11, defined as when the negative Niño4 is greater than 1 s.d. but less than 1.75 s.d. in amplitude (as shown in **d**); green dots indicate weak La Niña events, that is, 1984/85, 1995/96, 2000/01 and 2008/09, defined as when the negative Niño4 is greater than 0.5 s.d. but less than 1 s.d. in amplitude (as shown in **d**); red stars indicate extreme El Niño events, that is, 1982/83 and 1997/98, defined as when EOF1 is greater than 1 s.d. and negative EOF2 is greater than 1 s.d. in amplitude (as shown in panel **c**); purple dots indicate central-Pacific (CP) El Niño events, that is, 1990/91, 2002/03, 2004/05 and 2009/10, defined as when C-index is greater than 1 s.d. (as shown in **d**); yellow dots indicate events that are a mixture of central Pacific and eastern Pacific El Niño events, that is, 1979/80, 1986/87, 1987/88, 1991/92, 1994/95, 2001/02, 2003/04 and 2006/07, defined as when C-index is greater than 0.5 s.d. but less than 1 s.d. (as shown in **d**). **f–i**, Anomaly pattern of extreme El Niño, CP El Niño, extreme La Niña and weak La Niña, respectively.

that are outliers (Fig. 1d), exhibiting extraordinary warm anomalies inducing a massive rainfall increase in the eastern equatorial Pacific^{31,64,65}, without which the concept of EOF2 as an independent mode would have little basis²⁵.

The fact that the core of the ENSO SST anomaly varies longitudinally with event magnitude reflects the asymmetry and diversity of ENSO mechanisms. Nonlinear SST–wind feedback^{27,66} is thought to be a source of ENSO asymmetry: the response of zonal winds to warm SST anomalies is greater than to cold SST anomalies. On shorter timescales, stochastic forcing including westerly wind bursts (WWBs) is more tightly coupled with warm SST anomalies than with cold anomalies, and the interaction between WWBs and warm SST anomalies constitutes a positive feedback^{67,68}. Their coupling strengthens as the SST anomalies expand eastwards, in association with the eastward extension of the warm pool and reduced equatorial upwelling^{6,8,31}, contributing to a larger amplitude of positive SST anomalies in the eastern equatorial Pacific⁶⁸. For extreme El Niño, in addition to the initiation of this coupled process, as well as preconditioning by oceanic heat content³ and enhancement by off-equatorial atmospheric conditions³⁰, all linear positive feedbacks (zonal advection, Ekman pumping and thermocline feedback) play an important role in the growth of SST anomalies, and these processes strengthen as the anomaly centre moves eastward^{25,69}. The zonal advective feedback process in particular is enhanced by a reversal of the equatorial currents — a feature that characterises extreme El Niño events^{14,70}. At the mature phase, nonlinear vertical advection further contributes to the large positive SST anomalies⁷¹.

The large amplitude of warm anomalies attained during an extreme El Niño induces large changes in atmospheric circulation that lead to stronger discharge of the equatorial warm water volume, abruptly terminating the event and preconditioning for a La Niña²⁷. The associated thermocline shoaling in turn helps to produce a more efficient Bjerknes feedback through zonal SST gradient between the maritime region and the central Pacific³². Through nonlinear zonal advection (advection of anomalous zonal temperature gradient by anomalous zonal currents) and Ekman pumping, this leads to strong anomalous cooling in the central Pacific that signifies an extreme La Niña³². This also means that an extreme La Niña tends to develop following a strong El Niño. For central Pacific El Niño events, on the other hand, the thermocline variability and upwelling anomalies are weak, owing to the deep mean thermocline³³. There, the growth of SST anomalies is largely attributed to zonal advection, although smaller in magnitude than that in the eastern Pacific^{34,72,73}.

Recent understanding has led to a description of extreme El Niño and extreme La Niña that is both more dynamic and impact-focused, rather than solely focusing on SST anomalies at fixed locations. An extreme El Niño event features a reversal of the upper equatorial currents to flow eastward, facilitating an eastward propagation of SST anomalies¹⁴, a feature that is not seen during La Niña and weak El Niño events. During extreme El Niño events, the maximum total temperature is situated in the eastern equatorial Pacific. This weakens the meridional and zonal SST gradients, allowing the western Pacific convergence zone and the ITCZ to move to the eastern equatorial Pacific, an essential characteristic of an extreme El Niño event⁶⁴. This massive reorganization of the atmospheric circulation leads to a marked increase in rainfall in the eastern Pacific^{6,8,31}. The collapse of the mean meridional SST gradients also leads to the SPCZ swinging up to 1,000 km towards the Equator¹⁰. The use of atmospheric parameters, such as rainfall anomalies in the eastern equatorial Pacific or outgoing longwave radiation⁶⁵, to define an El Niño^{32,64}, for instance, has direct ties to both local and remote impacts; it has been proven to be of great utility for examining the extreme rainfall response of El Niño to greenhouse warming³¹, as underpinned by the nonlinearity of atmospheric response to ENSO SSTs.

Projected changes in extreme ENSO events

Despite lingering uncertainties, the future mean state changes are robustly produced by climate models. Although most models underestimate ENSO asymmetry³⁹, a subset of models can simulate asymmetric and nonlinear behaviour, such as the large precipitation increases over the eastern equatorial Pacific, zonal SPCZ and eastward propagation of warm SST anomalies that characterize the observed extreme El Niño, and the strong SST cooling over central Pacific associated with an extreme La Niña. As discussed further below, there is a robust projected increase in the frequency of such events, and this can be explained as consequences of the mean state changes^{10,14,31,32}.

But intermodel consensus continues to be weak in terms of changes in Niño3 SST anomalies. Out of 21 models that are able to produce extreme El Niño and extreme La Niña³², only 12 models produce an increase in ENSO amplitude (Fig. 2a). In association, only 12 models generate an increased frequency of extreme El Niño events, defined as Niño3 SST greater than 1.75 s.d. This is despite a tendency for more occurrences of extreme cold and warm anomalies (Fig. 2c). Using the nine models that are able to simulate the relative importance of ENSO linear feedbacks¹⁸ does not improve the consensus. The intermodel consensus is slightly better for the Niño4 SST anomalies: 15 out of the 21 (71%) models generate an increased amplitude (Fig. 2b), and 17 models produce an increased frequency in extreme La Niña, defined as when Niño4 SST is greater than a 1.75-s.d. value in amplitude, and similarly there is a tendency for more extreme cold and warm anomalies (Fig. 2d). The dynamics for the stronger consensus in Niño4 are not fully understood.

Given that extreme El Niño is characterized by a shift of the atmospheric convection to the eastern equatorial Pacific, a rainfall-based definition, for example as when Niño3 rainfall averaged over December to February (DJF) exceeds 5 mm day⁻¹, provides an alternative avenue for assessing the frequency of such extreme events³¹. Unless stated otherwise, this rainfall-based definition of extreme El Niño is used hereafter.

Climate models suggest that the relationship between changes in mean rainfall and ENSO amplitude is complex and may be time-varying. An increase in the eastern equatorial Pacific mean rainfall from the pre-industrial to the present day was found to be a good indicator of increased ENSO amplitude over the same period, but for reasons still unknown, such a linkage was found not to hold for changes from the present day to the later twenty-first century⁴³. On the other hand, background warming tends to increase the response of rainfall to SST anomalies because rainfall responds nonlinearly to the total temperature^{74,75}. As such, there is a strong intermodel consensus on the increased rainfall response to ENSO SST anomalies, even though there is a far weaker agreement on changes in those anomalies⁷⁵. The increased rainfall response to ENSO anomalies is not longitudinally uniform but has a maximum that shifts increasingly eastwards with stronger ENSO SST anomalies, associated with a faster background warming in the eastern than in the central equatorial Pacific^{10,74}.

Mean meridional and zonal SST gradients in the equatorial Pacific are barriers to movement of convection centres, and the enhanced warming in the eastern Pacific and equatorial regions weakens these barriers. The weakening mean SST gradients make it easier for a given positive SST anomaly to further weaken or even reverse the meridional (Fig. 3a,b) and zonal SST gradients, leading to increased occurrences of strong convection and high rainfall in the eastern equatorial Pacific^{31,64} (Box 1, features A and D), in spite of a convective threshold that is projected to increase with mean SSTs⁷⁶. Consequently, the frequency of extreme El Niño more than doubles, with a strong intermodel consensus. An analogous situation exists in the Indian Ocean, where anomalous conditions referred to as the positive Indian Ocean Dipole occur, featuring a shift of atmospheric convection to the west Indian Ocean. As a

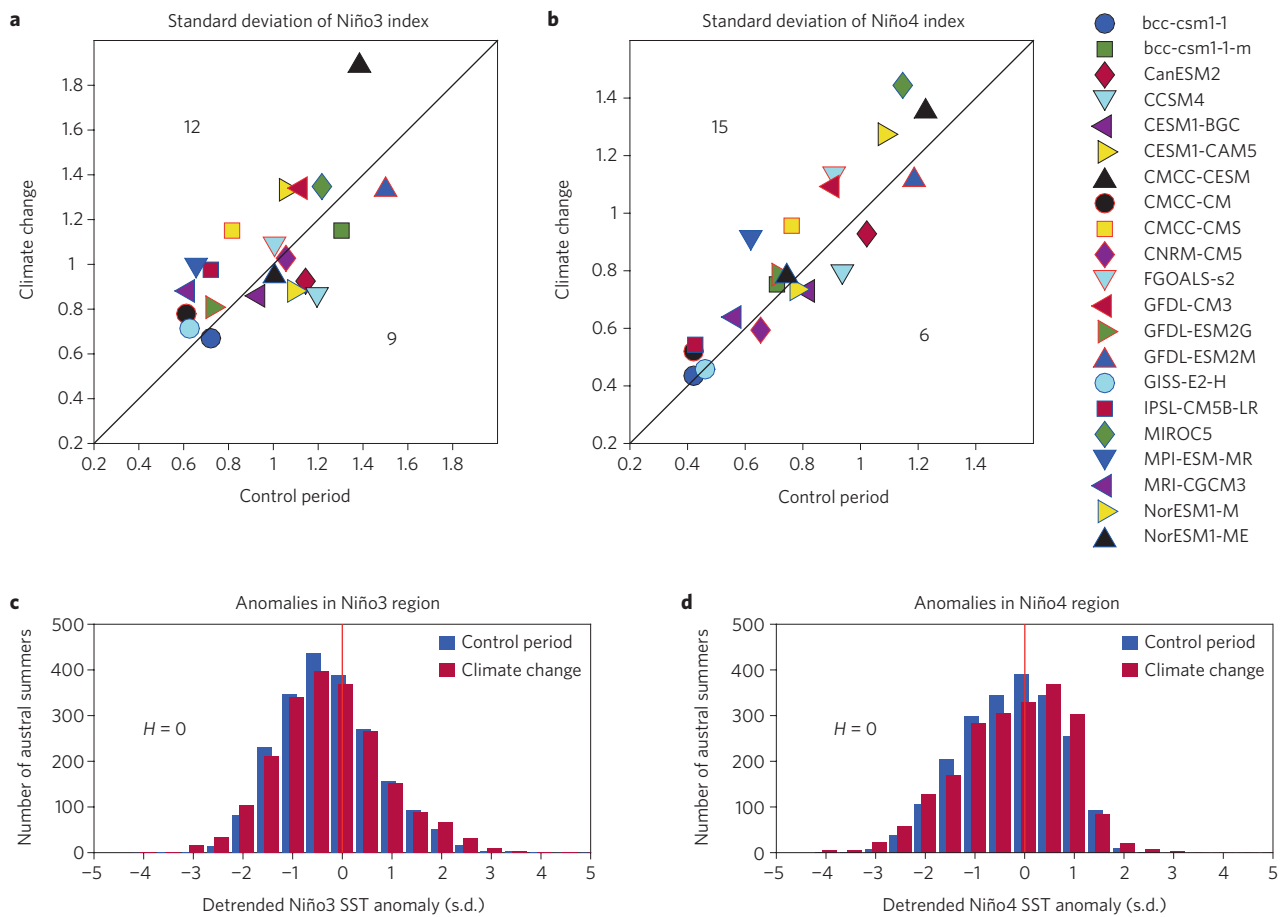


Figure 2 | Greenhouse-warming-induced changes in ENSO properties. The plots shown are based on outputs from CMIP5 experiments under historical and RCP8.5 scenarios using 21 models (out of 34 in total), focusing on austral summer (DJF). **a,b**, Comparison of Niño3 and Niño4 standard deviation (s.d) in the ‘Control’ period (1900–1999) (horizontal axis) and ‘Climate change’ period (2000–2099) (vertical axis). Numbers in the upper left indicate the number of models that produce an increase in s.d., and in the lower right, number of models that produce a decrease in s.d. **c,d**, Histogram of quadratically detrended Niño3 and Niño4 SST anomalies in s.d. for ‘Control’ period (1900–1999; blue) and ‘Climate change’ period (2000–2099; red). There is a tendency for each index to be more extreme in the ‘Climate change’ period, but the two histograms in each panel are not statistically different ($H = 0$) about the 95% confidence interval, according to a two-sided Student’s t -test.

result of the weakening Walker circulation, the west tropical Indian Ocean warms faster than the east. This leads to an increase in the frequency of extreme positive Indian Ocean Dipole events⁷⁷.

The projected weakening of westward mean upper-ocean currents in the equatorial Pacific^{40,78} leads to a doubling in El Niño events that feature prominent eastward propagation of SST anomalies¹⁴ (Box 1, feature A). Heat budget analysis shows that advection of temperature by the total current that is eastward contributes to eastward propagation of El Niño temperature anomalies¹⁴. Under global warming, the weakened mean current, associated with the weakened Walker circulation^{40,78}, favours occurrences of an eastward propagation, because it takes a smaller eastward anomaly during an El Niño to reverse the weaker westward mean current, leading to a doubling of eastward propagation events¹⁴. Unlike observed extreme El Niño events, however, not all modelled extreme El Niño events, identified using either rainfall-based or SST-based definition, correspond with eastward-propagating SST anomalies.

The projected faster warming in the equatorial than the off-equatorial Pacific^{39,41,53} is expected to lead to an increased frequency in zonal SPCZ events¹⁰ (Box 1, feature D). In the central and western equatorial Pacific, the warmest water of the warm pool is situated south of the Equator. This positive off-equatorial-minus-equatorial temperature gradient supports the southeastward extension of the SPCZ¹⁰. Because it is the meridional temperature

gradient that is important, zonal SPCZ events can occur without an extreme El Niño³¹. The projected warming pattern results in increased occurrences of diminishing meridional SST gradients, leading to an increased frequency of zonal SPCZ events.

In fact, the mean state changes concurrently favour an increased frequency of extreme El Niño, zonal SPCZ and eastward-propagating El Niño events, even though the dynamics for the increased frequency in each type of climate extreme are not necessarily exactly the same. As such, the frequency of any pairs of the three types of event more than doubles. Importantly, climate events similar to the 1982/83 and 1997/98 events, that is, with extreme rainfall anomalies in the eastern Pacific accompanied by a zonal SPCZ and eastward-propagating SST anomalies, are projected to double (Fig. 3a,b).

The projected increase in extreme El Niño events more frequently creates favourable conditions for the occurrence of extreme La Niña events, the frequency of which is expected to nearly double. The equatorial Pacific thermocline tends to shoal following an El Niño, helping a La Niña to develop³. This also allows more efficient Bjerknes feedback through Ekman pumping and nonlinear zonal advection — processes that are important for extreme La Niña³². Under greenhouse warming, such favourable conditions are further aided by mean state changes (Box 1, features A and B): the increased vertical temperature gradient is conducive to anomalous Ekman pumping. Faster warming over the maritime continent than in the

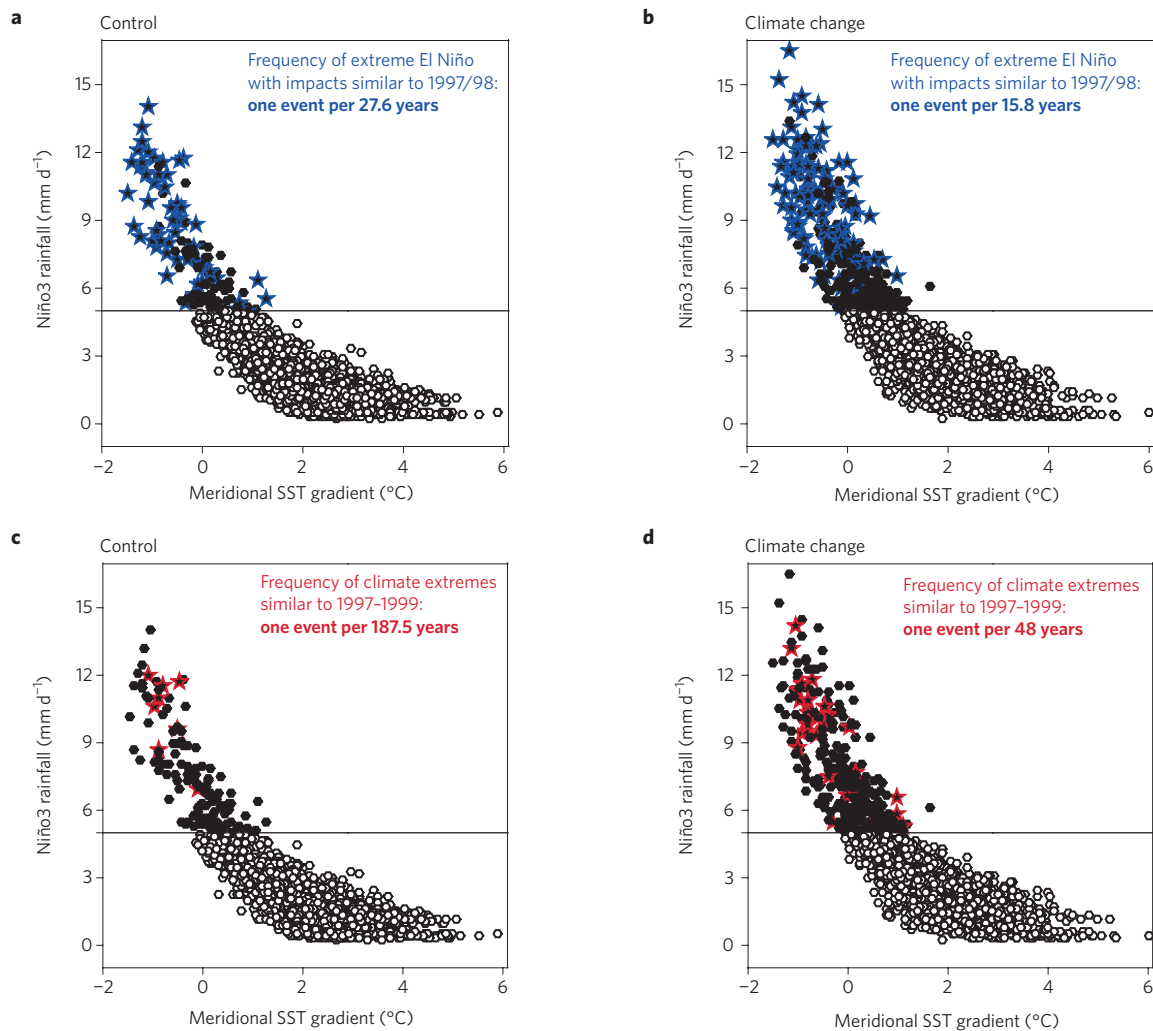


Figure 3 | Greenhouse-warming-induced changes in climate extremes. The plots shown are based on outputs from CMIP5 experiments under historical and RCP8.5 scenarios using 21 models (out of 34 in total), focusing on austral summer (DJF). In all panels, extreme El Niño is defined as when Niño3 rainfall is greater than 5 mm per day, marked by the horizontal line (ref. 31). **a,b**, Extreme El Niño events concurrent with eastward-propagating SST anomalies¹⁴ and zonal SPCZ events¹⁰ (blue stars), similar to the 1997/98 extreme El Niño event, for the 'Control' period (1900–1999) and 'Climate change' period (2000–2099), respectively. The frequency of such events almost doubles. **c,d**, Extreme El Niño events preceded by an extreme positive Indian Ocean Dipole, and followed by an extreme La Niña (red stars), similar to what happened in 1997–1999, for the 'Control' period (1900–1999) and 'Climate change' period (2000–2099), respectively.

central equatorial Pacific leads to more frequent occurrences of strong positive west-minus-east temperature gradients, anomalous easterlies, anomalous oceanic westward flow and upwelling, and therefore strong nonlinear zonal advection and Ekman pumping³². As a result, aggregated over models that are able to produce extreme El Niño and La Niña³², 75% of the increase in extreme La Niña occurs after an extreme El Niño event (defined using rainfall)³². Approximately 80% of these extreme El Niño events actually correspond with Niño3 SST anomalies exceeding an extreme threshold (1.75 s.d.), so some 60% of the increase occurs following an SST-defined extreme El Niño, analogous to the observed 1997/98 situation. The rest of the 15% occurs following an SST-defined moderate El Niño, like in 1988/89.

The projected increase in the frequency of extreme ENSO events is largely independent of a projected increased frequency of extreme positive Indian Ocean Dipole events⁷⁷, but the sequence of climate extremes similar to what the world experienced during 1997–1999, is projected to increase markedly, from one in 187 years to one in 48 years (Fig. 3c,d); during these two years, an extreme positive Indian Ocean Dipole preceded an extreme El Niño, and was then followed by an extreme La Niña.

ENSO teleconnection under greenhouse warming

ENSO teleconnections refers to the statistically significant ENSO-coherent fluctuations of a field remote from the central-to-eastern equatorial Pacific. In the tropical Pacific, atmospheric teleconnections are generated through a reorganization of atmospheric convection associated with ENSO SST anomalies that induce a deep baroclinic response⁷⁹. The effect is confined to the near-tropical portions of eastern Australia and western Pacific countries, leading to dry conditions in these regions but wet conditions in the eastern Pacific, during an El Niño. Outside the tropics, the same convective and diabatic atmospheric heating anomalies excite equivalent barotropic Rossby wave trains that propagate into the northern and southern extratropics⁸⁰. Referred to as the Pacific North American pattern⁸¹ and Pacific South American pattern⁸², respectively, these wave trains are the main agents for extratropical teleconnections. They generate changes to mid-latitude westerlies, thereby affecting rainfall through changes in mean state baroclinicity, steering of storms by the westerly jet streams, and possible orographic effects⁸³. There is so far no study suggesting that the way in which ENSO teleconnections operate will undergo fundamental changes.

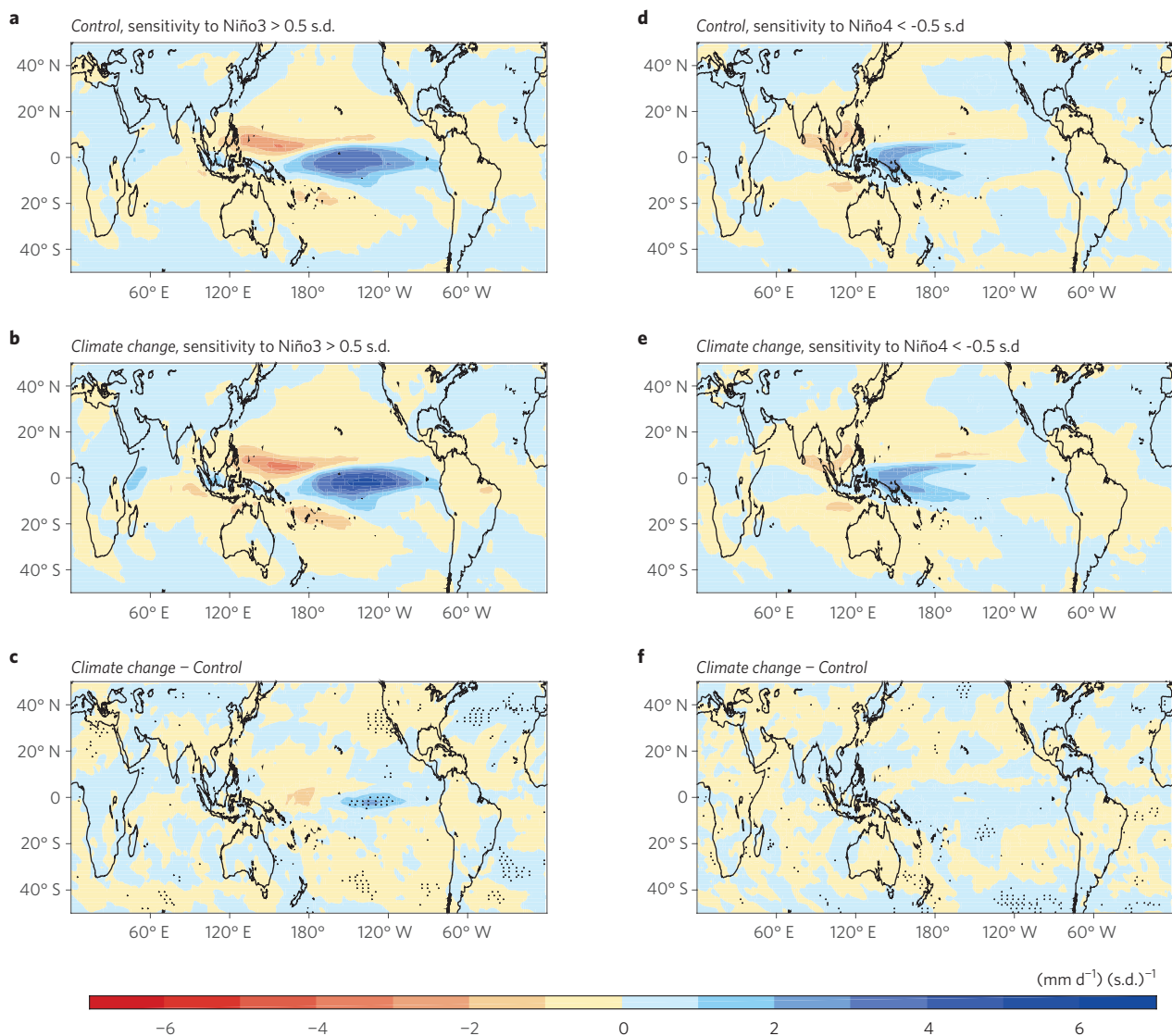


Figure 4 | Greenhouse-warming-induced change in rainfall response to Niño3 and Niño4 SST anomalies. Images shown are based on outputs from CMIP5 experiments under historical and RCP8.5 scenarios using 21 models (out of 34 in total), focusing on austral summer (DJF). **a, b**, Multi-model average of quadratically detrended rainfall anomalies associated with El Niño, obtained by regressing quadratically detrended rainfall anomalies onto quadratically detrended Niño3 using samples with Niño3 greater than positive 0.5 s.d., in ‘Control’ and ‘Climate change’ periods, respectively. **c**, The difference between **a** and **b** (that is, **b** – **a**). Stippling in **c** indicates regions where the difference is statistically significant above the 95% confidence level as determined by a two-sided Student’s *t*-test. Panels **d, e** and **f** are the same as **a, b** and **c**, respectively, but for the patterns associated with La Niña, using samples with a Niño4 greater than 0.5 s.d. in amplitude.

The nonlinearity of ENSO teleconnections should continue to operate with progressing greenhouse warming. Stemming from the strong asymmetry in the spatial anomaly pattern between El Niño and La Niña^{25,26,84,85} and between strong and moderate El Niño events^{22,24–26,29,66}, ENSO teleconnections are asymmetric with respect to extreme La Niña and extreme El Niño^{31,32}, and with respect to weak and strong events^{22,36,86}. This is underpinned by several features of tropical convection. First, atmospheric convection tends to occur where there are maximum SSTs exceeding the convective threshold (between 26 °C and 28 °C for the present-day climate)⁷⁶, so that an additional SST perturbation can generate convective available potential energy and thus increase the sensitivity of rainfall to SST perturbations. Second, during an extreme El Niño event, the atmospheric convection centre is displaced to the eastern equatorial Pacific³¹, in contrast to an extreme La Niña, for which convection, although suppressed in the central Pacific, is enhanced near its climatological position in the western Pacific³². Thus, in terms of the

convective anomaly pattern, and therefore far-field teleconnections, the asymmetry between extreme La Niña and extreme El Niño is far greater than that for tropical SST anomalies. A similar asymmetry is seen between a central Pacific El Niño and an extreme eastern Pacific El Niño, with the centre of enhanced convection located in the central equatorial Pacific for the central Pacific El Niño, but in the eastern equatorial Pacific for extreme El Niño^{31,36}. These asymmetric features are expected to persist in a warming climate.

Under greenhouse warming, the response of the tropical eastern Pacific rainfall anomalies, referenced to the changing mean state, to El Niño SST anomalies is likely to strengthen (Fig. 4), and the centre of maximum response to shift eastward^{31,75,87}. This is because rainfall responds nonlinearly to the absolute SST^{74,75}, increasing faster in the eastern than in the western Pacific. Outside the tropics, the Pacific North American pattern and the Aleutian low are expected to shift eastward, but there are reported variations on how the overall intensity of this teleconnection pattern may change^{87–90}, perhaps

in part linked to a lack of consensus on how ENSO SST amplitude will change.

Aggregated over models that are able to produce extreme El Niño and La Niña³², a stronger sensitivity of rainfall to positive Niño3 SST anomalies (Niño3 > 0.5 s.d.) in the future climate is seen in the eastern equatorial Pacific and some of the extratropical oceans (left column, Fig. 4), such that even if the amplitude of Niño3 SST variability does not change, the teleconnection has a tendency to increase in these regions. The response of rainfall to negative Niño4 SST anomalies ($|\text{Niño4}| > 0.5$ s.d.) shows, by and large, no significant change in either the tropics or the extratropics (right column, Fig. 4), and therefore the teleconnection will increase with the increased amplitude of Niño4 SST variability, which enjoys stronger intermodel agreement. As such, future extreme El Niño and La Niña events will occur more frequently^{31,32}, with at least a similar strength of teleconnection to that of the present-day events. The increased frequency of ENSO extremes is consistent with an increase in ENSO-related hydroclimate variability in the tropical Pacific region, particularly in regions such as southern Asia, with important implications because these regions are already severely stressed by variations in droughts, floods and crop yields⁹¹.

Summary, uncertainties and future research

The mean climate of the tropical Pacific is expected to change in the coming century as a result of ongoing emissions of greenhouse gases. Potential consequences of these mean state changes include more eastward-propagating El Niño events; an increased frequency of extreme El Niño events as defined using extreme rainfall in the eastern equatorial Pacific; a higher frequency of extreme La Niña events; an eastward shift of the ENSO rainfall teleconnection with a likely increased intensity; and more frequent extreme equatorward swings of large-scale convergence zones, such as the SPCZ and the ITCZ. Long records of palaeo-ENSO variance suggest that twentieth-century ENSO activity was significantly stronger than that during previous centuries^{92,93} or millennia⁹⁴. Because such palaeo-records typically document changes in both ENSO-related SST and rainfall anomalies, to varying degrees, the recent intensification of ENSO in these reconstructions provides some empirical support for the projections of more extreme ENSO events under greenhouse warming.

There are, however, known uncertainties that keep the confidence in these projections at the 'medium' level, following the IPCC definition. The projected weakening of the trade winds has been challenged by the observed strengthening over recent decades^{48,49,51}, although low-frequency variability can alter long-term trends, and the recent strengthening is probably associated with a negative IPO phase linked to the global warming hiatus^{50,52}. The projected increased frequency of extreme El Niño and extreme La Niña events is contingent upon the faster warming in the eastern equatorial Pacific Ocean. This is in turn a balance between processes that moderate easter Pacific warming, such as the ocean dynamical 'thermostat' mechanism⁹⁵, and those processes that enhance the warming, such as a reduced poleward heat transport¹⁶ and surface latent heat flux adjustment⁴¹. Despite some observational support of the expected enhanced equatorial eastern Pacific warming over the past 60 years, the tropical SST trend over the recent decades has featured suppressed warming in the east, contrary to the expected pattern from climate models.

The ability of climate models to realistically simulate the present-day mean state climate, ENSO properties and the associated teleconnection is another source of uncertainties. First, the common 'cold tongue'⁹⁶ and the double-ITCZ bias⁹⁷ in the mean state have persisted for decades, and every model suffers from its own intrinsic biases. Although in some cases models with a bias reduction produce an even higher frequency^{31,32}, the extent to which these biases are a source of uncertainty is yet to be tested. Second,

we still know little about how other important characteristics of ENSO will respond to greenhouse warming, such as interactions between ENSO and the annual cycle, termination and onset of El Niño events, coupling between WWBs and El Niño, and ENSO precursors and amplifying or damping mechanisms. Third, parameterization of sub-grid physics such as atmospheric convection, cloud formation and their coupling to the resolved dynamics remains inaccurate⁹⁸. Fourth, the genesis and evolution of ENSO can be affected by processes occurring in the Indian and Atlantic Oceans^{99,100}, but the associated processes are not well understood. An additional uncertainty is whether teleconnection patterns and intensity are correctly represented at regional scales, given that the regional impacts from ENSO extremes might not be resolved by present climate models.

Before a significant reduction in these uncertainties can be achieved, every effort must be made towards a projection that is consistent with our physical theoretical understanding and with what observations show. To this end, sustained ocean and atmospheric observations and effort to reduce errors are required to help determine the long-term changes in mean state and to validate ENSO simulations; efforts to reduce model biases in mean state, such as the 'cold tongue' bias, must be bolstered; and focused observational and modelling process studies for a fuller understanding of tropical convection, and cloud physics towards better parameterization for an improved ENSO simulation, must be strengthened. Although the biases and deficiencies may impede realistic simulation of ENSO extremes of the present-day and future climate, the likelihood of more frequent devastating ENSO extremes has a dynamical basis and should be considered as we prepare to face the consequences of greenhouse warming.

Received 30 March 2015; accepted 1 July 2015; published online 17 August 2015

References

- McPhaden, M. J., Zebiak, S. E. & Glantz, M. H. ENSO as an integrating concept in Earth science. *Science* **314**, 1740–1745 (2006).
- Neelin, J. D. *et al.* ENSO theory. *J. Geophys. Res.* **103**, 14261–14290 (1998).
- Jin, F.-F. An equatorial ocean recharge paradigm for ENSO. Part I: Conceptual model. *J. Atmos. Sci.* **54**, 811–829 (1997).
- Sun, D.-Z. El Niño: a coupled response to radiative heating? *Geophys. Res. Lett.* **24**, 2031–2034 (1997).
- Ropelewski, C. F. & Halpert, M. S. Global and regional scale precipitation patterns associated with the El Niño/Southern Oscillation. *Mon. Weath. Rev.* **115**, 1606–1626 (1987).
- Philander, S. G. H. Anomalous El Niño of 1982–83. *Nature* **305**, 16 (1983).
- Bove, M. C., O'Brien, J. J., Eisner, J. B., Landsea, C. W. & Niu, X. Effect of El Niño on US landfalling hurricanes, revisited. *Bull. Am. Meteorol. Soc.* **79**, 2477–2482 (1998).
- McPhaden, M. J. El Niño: The child prodigy of 1997–98. *Nature* **398**, 559–562 (1999).
- Wu, M. C., Chang, W. L. & Leung, W. M. Impact of El Niño–Southern Oscillation Events on tropical cyclone landfalling activities in the western North Pacific. *J. Clim.* **17**, 1419–1428 (2004).
- Cai, W. *et al.* More extreme swings of the South Pacific convergence zone due to greenhouse warming. *Nature* **488**, 365–369 (2012).
- Glynn, P. W. & de Weerd, W. H. Elimination of two reef-building hydrocorals following the 1982–83 El Niño. *Science* **253**, 69–71 (1991).
- Bell, G. D. *et al.* Climate assessment for 1998. *Bull. Am. Meteorol. Soc.* **80**, 1040–1040 (1999).
- McPhaden, M. J. & Zhang, X. Asymmetry in zonal phase propagation of ENSO sea surface temperature anomalies. *Geophys. Res. Lett.* **36**, L13703 (2009).
- Santoso, A. *et al.* Late-twentieth-century emergence of the El Niño propagation asymmetry and future projections. *Nature* **504**, 126–130 (2013).
- Valle, C. A. *et al.* The impact of the 1982–1983 El Niño–Southern Oscillation on seabirds in the Galapagos Islands, Ecuador. *J. Geophys. Res.* **92**, 14437–14444 (1987).
- Collins, M. *et al.* The impact of global warming on the tropical Pacific Ocean and El Niño. *Nature Geosci.* **3**, 391–397 (2010).
- DiNezio, P. N. *et al.* Mean climate controls on the simulated response of ENSO to increasing greenhouse gases. *J. Clim.* **25**, 7399–7420 (2012).

18. Kim, S.-T. *et al.* Response of El Niño sea surface temperature variability to greenhouse warming. *Nature Clim. Change* **4**, 786–790 (2014).
19. Taylor, K. E., Stouffer, R. J. & Meehl, G. A. An overview of CMIP5 and the experiment design. *Bull. Am. Meteorol. Soc.* **93**, 485–498 (2012).
20. Kug, J.-S., Ham, Y.-G., Lee, J.-Y. & Jin, F.-F. Improved simulation of two types of El Niño in CMIP5 models. *Environ. Res. Lett.* **7**, 034002 (2012).
21. Bellenger, H. *et al.* ENSO representation in climate models: From CMIP3 to CMIP5. *Clim. Dynam.* **42**, 1999–2018 (2014).
22. Hoerling, M. P., Kumar, A. & Zhong, M. El Niño, La Niña, and the nonlinearity of their teleconnections. *J. Clim.* **10**, 1769–1786 (1997).
23. Rodgers, K. B., Friederichs, P. & Latif, M. Tropical Pacific decadal variability and its relation to decadal modulations of ENSO. *J. Clim.* **17**, 3761–3774 (2004).
24. Yu, J.-Y. & Kim, S. T. Reversed spatial asymmetries between El Niño and La Niña and their linkage to decadal ENSO modulation in CMIP3 models. *J. Clim.* **24**, 5423–5434 (2011).
25. Takahashi, K., Montecinos, A., Goubanova, K. & Dewitte, B. ENSO regimes: Reinterpreting the canonical and Modoki El Niño. *Geophys. Res. Lett.* **38**, L10704 (2011).
- Proposes that the first two empirical orthogonal function modes of tropical Pacific sea surface temperature anomalies do not describe different phenomena (that is, El Niño–Southern Oscillation and ‘El Niño Modoki’) but rather the nonlinear evolution of ENSO.**
26. Takahashi, K. & Dewitte, B. Strong and moderate nonlinear El Niño regimes. *Clim. Dynam.* <http://dx.doi.org/10.1007/s00382-015-2665-3> (2015).
27. Choi, K.-Y., Vecchi, G. A. & Wittenberg, A. T. ENSO transition, duration, and amplitude asymmetries: role of the nonlinear wind stress coupling in a conceptual model. *J. Clim.* **26**, 9462–9476 (2013).
28. Timmermann, A. & Jin, F.-F. A nonlinear theory for El Niño bursting. *J. Atmos. Sci.* **60**, 152–165 (2003).
29. An, S.-I. & Jin, F.-F. Nonlinearity and asymmetry of ENSO. *J. Clim.* **17**, 2399–2412 (2004).
30. Hong, L.-C., LinHo & Jin, F.-F. A Southern Hemisphere booster of super El Niño. *Geophys. Res. Lett.* **41**, 2142–2149 (2014).
- Shows that preceding a super El Niño event is a transverse circulation characterized by a low-level equatorward flow, which spins off from a high sea-level-pressure anomaly around Australia and merges into the deep convection anomalies over the central Pacific, with westerly anomalies that reinforce the El Niño.**
31. Cai, W. *et al.* Increasing frequency of extreme El Niño events due to greenhouse warming. *Nature Clim. Change* **4**, 111–116 (2014).
32. Cai, W. *et al.* More frequent extreme La Niña events under greenhouse warming. *Nature Clim. Change* **5**, 132–137 (2015).
- Proposes that to examine dynamics associated with extreme La Niña, Niño4 surface temperature is a more appropriate index.**
33. Capotondi, A. *et al.* Understanding ENSO diversity. *Bull. Am. Meteorol. Soc.* **96**, 921–938 (2015).
- Uses observations, ocean reanalysis and climate models to provide a comprehensive review of dynamics associated with different ENSO types, and to show that the basic physical processes underlying the different ENSO types are not completely distinct.**
34. Kao, H. Y. & Yu, J. Y. Contrasting Eastern-Pacific and Central-Pacific types of ENSO. *J. Clim.* **22**, 615–632 (2009).
35. Yeh, S.-W. *et al.* El Niño in a changing climate. *Nature* **461**, 511–514 (2009).
36. Ashok, K., Behera, S. K., Rao, S. A., Weng, H. & Yamagata, T. El Niño Modoki and its possible teleconnection. *J. Geophys. Res.* **112**, C11007 (2007).
- Suggests that El Niño Modoki, with an anomaly centre in the central equatorial Pacific, is a different type of event independent from the canonical El Niño, which has an anomaly centre in the eastern equatorial Pacific.**
37. Hua, L., Yu, Y. & D.-Z. Sun, D.-Z. A further study of ENSO rectification: Results from an OGCM with a seasonal cycle. *J. Clim.* **28**, 1362–1382 (2015).
- Shows that the rectification effect of ENSO is to cool the western Pacific warm pool and warm the eastern equatorial Pacific.**
38. Sun, D.-Z., Zhang, T., Sun, Y. & Yu, Y. Rectification of El Niño–Southern Oscillation into climate anomalies of decadal and longer time-scales: Results from forced ocean GCM experiments. *J. Clim.* **27**, 2545–2561 (2014).
39. Liu, Z., Vavrus, S., He, F., Wen, N. & Zhong, Y. Rethinking tropical ocean response to global warming: The enhanced equatorial warming. *J. Clim.* **18**, 4684–4700 (2005).
40. Vecchi, G. A. *et al.* Weakening of tropical Pacific atmospheric circulation due to anthropogenic forcing. *Nature* **441**, 73–76 (2006).
41. Xie, S.-P. *et al.* Global warming pattern formation: Sea surface temperature and rainfall. *J. Clim.* **23**, 966–986 (2010).
42. An, S.-I., Kug, J.-S., Ham, Y.-G. & Kang, I.-S. Successive modulation of ENSO to the future greenhouse warming. *J. Clim.* **21**, 3–21 (2008).
43. Watanabe, M. *et al.* Uncertainty in the ENSO amplitude change from the past to the future. *Geophys. Res. Lett.* **39**, L20703 (2012).
44. Tokinaga, H., Xie, S.-P., Deser, C., Kosaka, Y. & Okumura, Y. M. Slowdown of the Walker circulation driven by tropical Indo-Pacific warming. *Nature* **491**, 439–443 (2012).
45. An, S.-I. *et al.* Recent and future sea surface temperature trends in tropical Pacific warm pool and cold tongue regions. *Clim. Dynam.* **39**, 1373–1383 (2012).
46. Luo, J. J., Sasaki, W. & Masumoto, Y. Indian Ocean warming modulates Pacific climate change. *Proc. Natl Acad. Sci. USA* **109**, 18701–18706 (2012).
47. McGregor, S. *et al.* Recent Walker circulation strengthening and Pacific cooling amplified by Atlantic warming. *Nature Clim. Change* **4**, 888–892 (2014).
48. Solomon, A. & Newman, M. Reconciling disparate twentieth-century Indo-Pacific ocean temperature trends in the instrumental record. *Nature Clim. Change* **2**, 691–699 (2012).
49. Dong, B. W. & Lu, R. Y. Interdecadal enhancement of the Walker circulation over the Tropical Pacific in the late 1990s. *Adv. Atmos. Sci.* **30**, 247–262 (2013).
50. England, M. H. *et al.* Recently intensified Pacific Ocean wind-driven circulation and the ongoing warming hiatus. *Nature Clim. Change* **4**, 222–227 (2014).
51. L’Heureux, M., Lee, S. & Lyon, B. Recent multidecadal strengthening of the Walker circulation across the tropical Pacific. *Nature Clim. Change* **3**, 571–576 (2013).
52. Kosaka, Y. & Xie, S.-P. Recent global-warming hiatus tied to equatorial Pacific surface cooling. *Nature* **501**, 403–407 (2013).
53. Timmermann, A., McGregor, S. & Jin, F.-F. Wind effects on past and future regional sea level trends in the Southern Indo-Pacific. *J. Clim.* **23**, 4429–4437 (2010).
54. McPhaden, M. J., Lee, T. & McClurg, D. El Niño and its relationship to changing background conditions in the tropical Pacific Ocean. *Geophys. Res. Lett.* **38**, L15709 (2011).
55. Wittenberg, A. T., Rosati, A., Delworth, T. L., Vecchi, G. A. & Zeng, F. ENSO modulation: Is it decadal predictable? *J. Clim.* **27**, 2667–2681 (2014).
56. Xiang, B., Wang, B. & Li, T. A new paradigm for the predominance of standing Central Pacific warming after the late 1990s. *Clim. Dynam.* **41**, 327–340 (2013).
57. An, S.-I. & Wang, B. Interdecadal change of the structure of the ENSO mode and its impact on the ENSO frequency. *J. Clim.* **13**, 2044–2055 (2000).
58. Fedorov, A. & Philander, S. G. Is El Niño changing? *Science* **288**, 1997–2002 (2000).
59. Zhang, T. & Sun, D.-Z. ENSO Asymmetry in CMIP5 models. *J. Clim.* **27**, 4070–4093 (2014).
- Shows that most models underestimate ENSO asymmetry, and that the underestimation primarily results from a weaker SST warm anomaly over the eastern Pacific and a westward shift of the centre of the anomaly.**
60. Ohba, M. & Ueda, H. Role of nonlinear atmospheric response to SST on the asymmetric transition process of ENSO. *J. Clim.* **22**, 177–192 (2009).
61. Okumura, Y. M. & Deser, C. Asymmetry in the duration of El Niño and La Niña. *J. Clim.* **23**, 5826–5843 (2010).
62. Burgers, G. & Stephenson, D. B. The ‘normality’ of El Niño. *Geophys. Res. Lett.* **26**, 1027–1030 (1999).
63. Trenberth, K. E. & Stepaniak, D. P. Indices of El Niño evolution. *J. Clim.* **14**, 1697–1701 (2001).
64. Lengaigne, M. & Vecchi, G. A. Contrasting the termination of moderate and extreme El Niño events in Coupled General Circulation Models. *Clim. Dynam.* **35**, 299–313 (2010).
- Proposes that a large rainfall anomaly in the eastern equatorial Pacific can be used to examine whether a model is able to generate an extreme El Niño.**
65. Chiodi, A. M. & Harrison, D. E. El Niño impacts on seasonal US atmospheric circulation, temperature, and precipitation anomalies: The OLR-event perspective. *J. Clim.* **26**, 822–837 (2013).
- Shows that since 1979 most of the US seasonal weather impact of El Niño events has been associated with the few events identified by the behaviour of outgoing longwave radiation (OLR) over the eastern equatorial Pacific, suggesting the utility of OLR to define El Niño.**
66. Frauen, C. & Dommengat, D. El Niño and La Niña amplitude asymmetry caused by atmospheric feedbacks. *Geophys. Res. Lett.* **37**, L18801 (2010).
67. Gebbie, G., Eisenman, I., Wittenberg, A. & Tziperman, E. Modulation of westerly wind bursts by sea surface temperature: A semistochastic feedback for ENSO. *J. Atmos. Sci.* **64**, 3281–3295 (2007).
68. Lengaigne, M. *et al.* The March 1997 Westerly Wind Event and the onset of the 1997/98 El Niño: Understanding the role of the atmospheric response. *J. Clim.* **16**, 3330–3343 (2003).
69. An, S.-I. & Jin, F.-F. Collective role of thermocline and zonal advective feedbacks in the ENSO mode. *J. Clim.* **14**, 3421–3432 (2001).
70. Kim, W. & Cai, W. The importance of the eastward zonal current for generating extreme El Niño. *Clim. Dynam.* **42**, 3005–3014 (2014).
- Finds that the eastward zonal current, seen only during extreme El Niño, plays an important role in making an El Niño event extreme.**

71. Jin, F.-F., An, S.-I., Timmermann, A. & Zhao, J. Strong El Niño events and nonlinear dynamical heating. *Geophys. Res. Lett.* **30**, 1120 (2003).
72. Lübbecke, J. & McPhaden, M. J. Assessing the twenty-first-century shift in ENSO variability in terms of the Bjerknes stability index. *J. Clim.* **27**, 2577–2587 (2014).
73. Newman, M., Alexander, M. A. & Scott, J. D. An empirical model of tropical ocean dynamics. *Clim. Dynam.* **37**, 1823–1841 (2011).
74. Chung, C. T. Y., Power, S. B., Arblaster, J. M., Rashid, H. A. & Roff, G. L. Nonlinear precipitation response to El Niño and global warming in the Indo-Pacific. *Clim. Dynam.* **42**, 1837–1856 (2013).
75. Power, S. B., Delage, F., Chung, C. T. Y., Kociuba, G. & Keay, K. Robust twenty-first century projections of El Niño and related precipitation variability. *Nature* **502**, 541–547 (2014).
76. Johnson, N. C. & Xie, S.-P. Changes in the sea surface temperature threshold for tropical convection. *Nature Geosci.* **3**, 842–845 (2010).
Demonstrates that under global warming, surface temperature threshold for tropical atmospheric convection increases commensurately with mean temperature over the tropics.
77. Cai, W. *et al.* Increased frequency of extreme Indian Ocean Dipole events due to greenhouse warming. *Nature* **510**, 254–258 (2014).
78. Sen Gupta, A., Ganachaud, A., McGregor, S., Brown, J. N. & Muir, L. Drivers of the projected changes to the Pacific Ocean equatorial circulation. *Geophys. Res. Lett.* **39**, L09605 (2012).
79. Gill, A. E. Some simple solutions for heat-induced tropical circulation. *Q. J. R. Meteorol. Soc.* **106**, 447–462 (1980).
80. Hoskins, B. J. & Karoly, D. J. The steady linear response of a spherical atmosphere to thermal and orographic forcing. *J. Atmos. Sci.* **38**, 1179–1196 (1981).
81. Horel, J. D. & Wallace, J. M. Planetary-scale atmospheric phenomena associated with the Southern Oscillation. *Mon. Weath. Rev.* **109**, 813–829 (1981).
82. Karoly, D. J. Southern Hemisphere circulation features associated with El Niño–Southern Oscillation events. *J. Clim.* **2**, 1239–1252 (1989).
83. Cai, W., van Rensch, P., Cowan, T. & Hendon, H. H. Teleconnections pathways of ENSO and IOD and the mechanisms for impacts on Australian rainfall. *J. Clim.* **24**, 3910 (2011).
84. Okumura, Y. M., Ohba, M., Deser, C. & Ueda, H. A proposed mechanism for the asymmetric duration of El Niño and La Niña. *J. Clim.* **24**, 3822–3829 (2011).
85. DiNezio, P. N. & Deser, C. Nonlinear controls on the persistence of La Niña. *J. Clim.* **27**, 7335–7355 (2014).
86. Zhang, W. J., Jin, F.-F., Ren, H.-L., Li, J. & Zhao, J.-X. Differences in teleconnection over the North Pacific and rainfall shift over the USA associated with two types of El Niño during boreal autumn. *J. Meteorol. Soc. Jpn* **90**, 535–552 (2012).
87. Kug, J.-S., An, S.-I., Ham, Y.-G. & Kang, I.-S. Changes in El Niño and La Niña teleconnections over North Pacific-America in the global warming simulations. *Theor. Appl. Climatol.* **100**, 275–282 (2010).
88. Meehl, G. A. & Teng, H. Multi-model changes in El Niño teleconnections over North America in a future warmer climate. *Clim. Dynam.* **29**, 779–790, (2007).
89. Stevenson, S. L. Significant changes to ENSO strength and impacts in the twenty-first century: Results from CMIP5. *Geophys. Res. Lett.* **39**, L17703 (2012).
90. Zhou, Z.-Q. *et al.* Global warming-induced changes in El Niño teleconnections over the North Pacific and North America. *J. Clim.* **27**, 9050–9064 (2014).
91. Seager, R., Naik, N. & Vogel, L. Does global warming cause intensified interannual hydroclimate variability? *J. Clim.* **25**, 3355–3372 (2012).
92. McGregor, S., Timmermann, A., England, M. H., Elison Timm, O. & Wittenberg, A. T. Inferred changes in El Niño–Southern Oscillation variance over the past six centuries. *Clim. Past* **9**, 2269–2284 (2013).
93. Li, J. *et al.* El Niño modulations over the past seven centuries. *Nature Clim. Change* **3**, 822–826 (2013).
94. Cobb, K. M. *et al.* Highly variable El Niño–Southern Oscillation throughout the Holocene. *Science* **339**, 67–70 (2013).
95. Cane, M. A. *et al.* Twentieth century sea surface temperature trends. *Science* **275**, 957–960 (1997).
96. Li, G. & Xie, S.-P. Tropical biases in CMIP5 multimodel ensemble: The excessive equatorial Pacific cold tongue and double ITCZ problems. *J. Clim.* **27**, 1765–1780 (2014).
97. Bellucci, A., Gualdi, S. & Navarra, A. The double-ITCZ syndrome in coupled general circulation models: The role of large-scale vertical circulation regimes. *J. Clim.* **23**, 1127–1145 (2009).
98. Bony, S. & Dufresne, J. L. Marine boundary layer clouds at the heart of tropical cloud feedback uncertainties in climate models. *Geophys. Res. Lett.* **32**, L20806 (2005).
99. Izumo, T. *et al.* Influence of the state of the Indian Ocean Dipole on the following year's El Niño. *Nature Geosci.* **3**, 168–172 (2010).
100. Ham, Y. G., Kug, J. S., Park, J. Y. & Jin, F. F. Sea surface temperature in the north tropical Atlantic as a trigger for El Niño/Southern Oscillation events. *Nature Geosci.* **6**, 112–116 (2013).

Acknowledgements

W.C. and G.W. are supported by the Australian Climate Change Science Program and a CSIRO Office of Chief Executive Science Leader award. A.S. is supported by the Australian Research Council. M.C. was supported by NERC NE/I022841/1. S.W.Y. is supported by the National Research Fund of Korea grant funded by the Korean Government (MEST) (NRF-2009-C1AAA001-2009-0093042). S.I.A. was supported by the Basic Science Research Program through the National Research Foundation of Korea funded by the Ministry of Science, ICT and Future Planning (No. 2014R1A2A1A11049497). This is PMEL contribution number 4038.

Author contributions

W.C., A.S., G.W. and S.W.Y. wrote the initial version of the paper. G.W. performed the model output analysis and generated all figures. All authors contributed to interpreting results, discussion of the associated dynamics and improvement of this paper.

Additional information

Reprints and permissions information is available online at www.nature.com/reprints. Correspondence should be addressed to W.C.

Competing financial interests

The authors declare no competing financial interests.